International Journal of Nanoelectronics and Materials
Volume 16 (Special Issue) December 2023 [253-266]

The Encouragement of Graphite and Graphene Oxide Particles on Corrosion Protection Properties for Polyurethane Palm Oil Based UV Curable Coating

Mohd Sofian Alias[1,2], Norinsan Kamil Othman[1,*], Siti Radiah Mohd Kamarudin[3], Siti Fatahiyah Mohamad[2], Mohd Hamzah Harun[2], Mahathir Mohamed[2], T. Rida[2], Khairul Azhar Abdul Halim[2], Zaifol Samsu[3] , Nur Ubaidah Saidin[3] dan Norhasimah Alias[4]

[1]Materials Science Programme, Department of Applied Physics, Universiti Kebangsaan Malaysia, Bangi, 43600 Selangor, Malaysia
[2]Radiation Processing Technology Division, Malaysian Nuclear Agency, Bangi, 43000 Kajang, Selangor, Malaysia
[3]Materials Technology Group, Malaysian Nuclear Agency, Bangi,43000 Kajang, Selangor, Malaysia
[4]Centre for Foundation, Language and General Studies, University of Cyberjaya, 63000 Cyberjaya, Selangor, Malaysia

ABSTRACT

This research explores the impact of derivative graphite additives in enhancing the corrosion prevention system of UV curable polyurethane coatings based on palm oil. UV irradiation technique was used in this study to produce cured protection coating. Two types of particles, respectively graphite and graphene oxide were used to understand the differential of both particles in physicomechanical behaviour of the curable coating. The study delves into the formulation and characterization of these coatings, assessing their effectiveness in preventing corrosion. The polymerisation effect by UV irradiation and influence of filler (graphene oxide and graphite) on physical properties of coating were studied by using Fourier Transform Infrared Spectroscopy (FTIR) and gel content together with hardness test. Besides that, X-ray Diffraction (XRD) and Field emission scanning electron microscopy (FESEM) were used to investigate the morphology of curable coating. Meanwhile Electro impedance spectroscopy (EIS) and contact angle measurement were carried out to investigate the related behaviour on corrosion protection properties. All the results were concluded to explain the role of graphite and graphene oxide in curable coating crosslink network. The finding in this study indicates that tortuosity structured which formed by graphite and graphene oxide in UV curable coating matrix were successfully retard corrosion rate per year on mild steel from 31.24 mpy to 43.91 x 10^{-6} mpy. This work aims to provide valuable insights into the development of eco-friendly and efficient corrosion protection solutions in the realm of coatings and materials science.

Keywords: Derivative graphite, palm oil, corrosion protection, UV curable coating

1. INTRODUCTION

Polyurethane is a versatile polymer that can be synthesized from oil-based sources like vegetable oils, castor oil, or other renewable feedstocks. These oil-based polyurethanes serve as the main component of the coating [1]. Polyurethane is preferred as a coating material for various applications due to its exceptional combination of properties such as weather resistance, chemical resistance, fast cure, good adhesion etc. Nowadays people are looking for environmentally friendly products due to new regulations which are introduced in most countries in the world and also awareness in the community. One of interesting and potential products in this scope is UV curable corrosion protection coating. UV curable coating is one of

* Corresponding authors: insan@ukm.edu.my

superior products which is used in protect metal surface from corrosion damage. Corrosion protection polymer coatings are specialized coatings applied to surfaces, typically metal, to prevent or reduce the degradation of the substrate material due to corrosion. These coatings are designed to provide a barrier between the substrates and corrosive environments, thereby extending the lifespan of the protected material. Corrosion protection coatings made from bio-based polyurethane are a type of coating designed to prevent or reduce the corrosion of metallic surfaces while incorporating bio-based or renewable materials in their composition. These coatings offer environmental benefits compared to traditional coatings that rely on petrochemical-derived materials. Here's an overview of how oil- based polyurethane corrosion protection coatings work.

Much research has been done in this field in order to optimize and find the best formulation which finally can be as an alternative product to replace petrochemical based. Recently the polyurethane oil-based coating resin has been successfully synthesized from sunflower oil via two-step process epoxidation. The coating was effectively enhanced with the addition of reduced graphene oxide in oil-based polyurethane. [2]. Meanwhile previous study revealed that amorphous and good conductive polyurethane film can be synthesized from castor oil via transesterification process [3]. Meanwhile preparation of hyperbranched oil-based polyurethane from castor oil and dimethylol propionic acid (DMPA) was proven in producing highly density crosslink network with good mechanical properties of coating polymer [4].

More specific work in corrosion protection coating from oil based was successfully reported on synthesis bio-based polyurethane from crambe oil and castor oil incorporated with Zn micro flake. EIS result indicated corrosion resistance improved with the highest content of Zn micro-flakes [5]. The study of thermoset anticorrosion polyurethane coating by using lignin-based revealed a well dispersion and formation of crosslink network give superior corrosion resistance than other reported bio-based polymer coatings. These results demonstrate that the synthesis of highly reactive lignin-based polyols based on thiol-ene chemistry is an effective and facile strategy, which is vital for the development of high-performance bio-based polyurethane anticorrosive coatings [6]. Meanwhile water-based polyurethane was successfully prepared from Sorbitan monooleate polyol demonstrated excellent mechanical and corrosion protection properties due to the presence of large amounts of hydrogen bonding and rigid furan ring, and high crosslinking densities [7].

Another interesting approach in enhanced the corrosion protection properties was by included the graphite and graphene oxide particles in coating resin formulation. The influence of graphite particles in preventing the corrodent agent mobility was completely studied by using EIS. The results showed the presence of graphite particles were successfully developed dense polymer matrix which slow down the penetration of corrodent agents onto the metal surface [8]. Another study also reported that addition of graphite particles at 80 % in epoxy coating will give good compactness of the coating and increase the corrosion resistance of the composite organic layer [9]. Meanwhile, graphene oxide particles also demonstrated a good performance in corrosion protection properties. The covalently modified graphene oxide gives well dispersibility, thus reducing defects and voids to greatly enhance the interfacial interaction between polymer matrix. As a result, the presence of graphene oxide developed dense structure in polymer matrix towards superior corrosion protection performance [10]. Furthermore, previous study showed the modification of graphene oxide with diamine will increase hydrophobicity and barrier properties of epoxy coating. The amino functionalized graphene oxide increased the ionic resistance of the coating through reacting with OH- and prevented the Cl- ions diffusion into the coating body consequently retarded corrosion process. [11]

Regarding previous worked, it was clearly described that oil-based polyurethane coating could significantly improve the performance of the coating and can be potentially candidate to replace petrochemical product towards green technology. Previous results also indicate that oil-based polyurethane gives a good value for corrosion protection properties. In order to develop green and eco-friendly corrosion protection coating, in this work the type of filler (graphite and graphene oxide) were formulated in palm oil-based urethane acrylate resin. UV irradiation was applied in curing process and performance of cured film were analyzed with several scientific equipment.

In this work, the role of graphene oxide and graphite in POBUA to protect mild steel surface were investigated and briefed.

2. MATERIAL AND METHODOLOGY

2.1 Materials

Commercially, mild steel with the following composition by weight was obtained: 0.001% phosphorus (P), 0.045% aluminum (Al), 0.187% silicon (Si), 0.586% manganese (Mn), 0.486% carbon (C), 0.004% sulfur (S), and 98.691% iron (Fe). The steel was received and then cut into pieces (4 cm x 4 cm). Palm oil-based urethane acrylate (POBUA) supplied by Nuclear Malaysia was used without any additional processing. Additionally, graphene oxide particles were used as filler in POBUA, obtained from Timesnano. Graphite particles which also used as filler for comparison study was supply from Radiation Technology Division, Nuclear Malaysia. Meanwhile, the photoinitiator Irgacure 184, also known as alpha-hydroxy ketone chemically, was purchased from Sigma Aldrich.

2.2 Preparation of UV- curable POBUA Composite Coating

The UV-curable formulation resin from POBUA (Palm oil-based urethane acrylate) was comprised of three primary material: oligomer, filler, and photoinitiator. As comparison study Graphene oxide and graphite particles employed as a filler, was incorporated into the POBUA oligomer at 0.5wt.% weight percentages. To initiate the UV polymerization process, 5% wt. photoinitiator was added to each formulation, which had a total weight of 40 grams. At first, POBUA resin was poured into an amber bottle, and the measured weight of the graphite filler was combined with the POBUA resin. The mixture was stirred at a speed of 300 rpm for 2 hours. Following that, a sonicator (VCX500 by Sonics & Materials, USA) was utilized to sonicate and disperse the filler in the POBUA resin at a power of 500W and a frequency of 20 kHz. The amplitude and pulses were set at 50%, with a 1-second stop for every 2-second interval, lasting for 10 minutes. All POBUA/GOP formulations were exposed to UV light after being stored for 24 hours at a temperature of 27°C. To protect the mild steel surface, the formulation was applied to 4 cm x 4 cm mild steel plates using a K Hand Coater with a roller wire diameter of 0.64 mm, resulting in a film thickness of 50 μm. Subsequently, wet films were cured using a 20 cm-wide IST UV machine, operated at a current of 8A and a conveyor speed of 10 m/min for 6 passes. Finally, all cured films were peeled off from the mild steel surface for characterization through spectroscopic, hardness and morphology testing.

Table 1 Weight composition used in this work

Sample	Oligomer (POBUA) (g)	Graphite (g)	Graphene Oxide (g)	Irgacure184 (g)
POBUA	40	0	0	2
POBUA + 0.5 wt Graphite	40	0.2	0	2
POBUA + 0.5 wt Graphene Oxide	40	0	0.2	2

2.3 Characterization

The curing process under UV irradiation was continuously observed using FTIR spectrophotometry (Bruker Tensor II, Spectrum 2000). All spectra were obtained using the attenuated total reflection (ATR) method. A total of 32 scans were collected within a wavenumber range of 500–4000 cm^{-1}, with a resolution of 4.0 cm^{-1} for all recorded spectra. Furthermore, the crystalline properties of the POBUA/filler were analyzed using X-ray powder diffractometry (PANalytical X'Pert PRO MPD PW 3040/60), which utilized Ni-filtered Cu Kα radiation (λ = 0.15418 nm). The diffraction data were collected at 50 kV and 120 mA, with a scanning speed of 0.02° and 6.5° per minute, covering 2θ values ranging from 5° to 60°. To determine the crystallinity index of POBUA/Graphene oxide, the Segal equation (12) was employed, as shown below:

$$Crystalinity\ Index\ (\%) = \frac{I_{(002)} - I_{am}}{I_{(002)}} \quad (1)$$

In this study, the surface properties of UV-curable coatings were examined using scanning field emission scanning electron microscopy (FESEM), specifically the Carl Zeiss/GeminiSEM 500, operated at 3 kV with a magnification of 50,000x. The images were processed using Aztec software. Prior to FESEM imaging, samples were coated with platinum to prevent charging. Additionally, the wetting behavior of the curable coatings was assessed using contact angle (CA) measurements. CA measurements for distilled water droplets were recorded for each prepared sample using an optical contact angle device from Biolin Scientific (Finland). For CA inspection, images of 5 µL droplets of distilled water that were horizontally placed on the sample holder were captured to determine the static CA. The contact angle values for water droplets on the left and right sides of the curable coating surface, with an accuracy of 0.1°, were determined using the Young-Laplace fitting method with Attension Theta software. All measurements were performed in triplicate at an ambient room temperature of 30 ± 2°C. To assess the performance of the polymerized polymer after UV irradiation, the cured film was extracted in a Soxhlet extractor using acetone as the solvent and then dried until a constant weight was achieved. The hardness of the polymerized coating film was measured using a pendulum hardness tester, specifically the TQC Sheen model from the Netherlands, following the ISO 1522 standard method, known as the König test method. The percentage of pendulum hardness oscillation (PH%) relative to the glass standard was used to represent the coating's hardness performance.

2.4 Corrosion Performance Analysis of POBUA Composite Coatings

The corrosion resistance of the coatings was assessed in a 3.5% sodium chloride (NaCl) solution using electrochemical measurement techniques, specifically electrochemical impedance spectroscopy (EIS) and Tafel polarization curve analysis. To conduct these tests, a Reference 600 Potentiostat/Galvanostat/ZRA from Gamry Instruments in the USA was connected to a computer equipped with Gamry Framework software. During testing, the impedance of the coating was measured, and the Tafel polarization curve was recorded with respect to a saturated calomel reference electrode (SCE). The corrosion testing setup consisted of approximately 300 mL of

3.5% NaCl solution prepared using de-ionized water. The three-electrode system comprised the coated specimen as the working electrode, a graphite rod as the counter electrode, and SCE as the reference electrode. The exposed surface area of the coated steel was 1 cm2. All measurements were conducted in a naturally aerated NaCl solution at room temperature. Prior to conducting EIS and Tafel polarization measurements, the open circuit potential (Eoc) value was monitored against the SCE reference electrode for one hour. For EIS measurements, the tests were carried out at the open circuit potential using a sinusoidal amplitude of 10 mV Root Mean Square (RMS) and 10 data points per decade, covering a frequency range from 0.01 Hz to 100 kHz. Tafel polarization curves were generated with a scanning rate of 0.125 mV/s, starting from an initial potential 250 mV below Eoc and ending at a final potential 250 mV above Eoc. To analyze the collected data, the Gamry Echem Analyst software was employed.

3. RESULT AND DISCUSSION

3.1 Influence of Graphite and Graphene Oxide on Hardness and Polymerisation Process

Crosslink network formation is vital in developing the best protection coating for mild steel surfaces. The density of crosslink network will affect the hardness and pathway of corrodent agent. Since UV curable coating properties were depending by the conversion of acrylate group it was very important to monitor the polymerization process via FTIR analysis [12]. In this study the conversion of Carbon double bond (C=C) in POBUA was observed at 810 cm^{-1} [10]. The results showed the spectrum of acrylate group clearly disappeared after UV irradiation exposure on POBUA resin. The photoinitiator absorbed UV radiation energy before the polymerization process undertaken between free radical and acrylate group. The completion of curing process can also be observed by transforming the liquid resin into solid coating [13].

Table 2 Hardness and Gel Fraction of POBUA, POBUA +0.5 % Graphite and POBUA+ Graphene Oxide 0.5 wt%

Sample	Hardness index	Gel Fraction
POBUA	8	85
POBUA + 0.5 wt% Graphite	12	87
POBUA + 0.5 wt% Graphene oxide	12	88

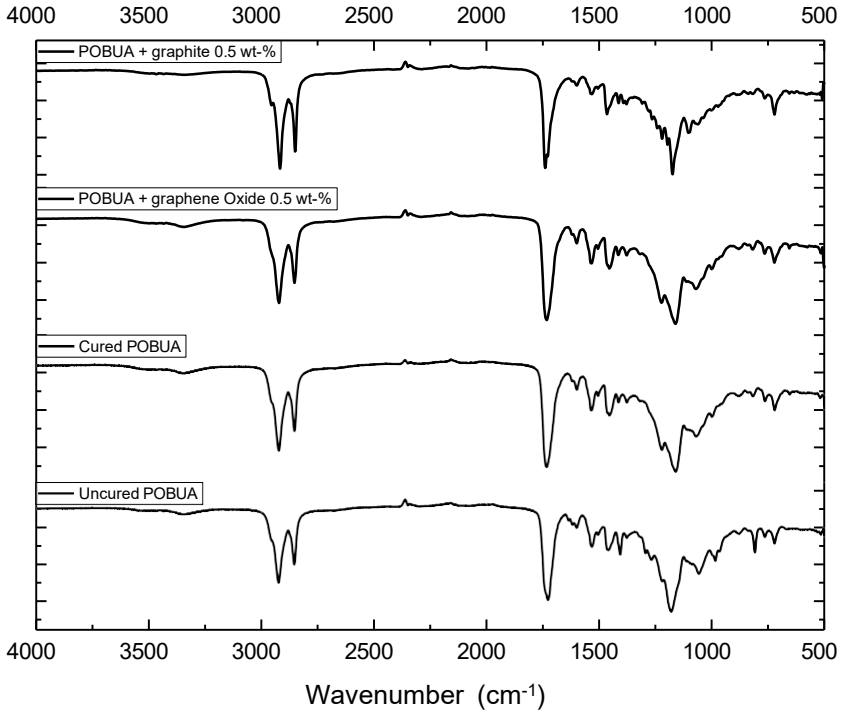

Figure 1. Overlay of FTIR spectrum for POBUA uncured, POBUA cured, POBUA + graphene oxide 0.5 wt. %, POBUA graphite 0.5 wt. %.

Furthermore, both spectrum POBUA + 0.5 wt. % graphite and POBUA + 0.5 wt. % graphene oxide signed the shifting of spectrum to lower energy at around 1200cm^{-1} to 1100cm^{-1}. This was contribution from the weak force in POBUA molecules (such as hydrogen bonding and van der waals) which occurred between both type of graphite particles (graphene oxide and graphite).

Meanwhile table 1 revealed, graphite particles (graphite and Graphene oxide) give slight improvement on curable POBUA coating strength. Regarding Figure 2, FEESEM image displays a good dispersion of both graphite particles in POBUA matrix which physically bonded towards preventing the deformation of polymer from molecules movement by external force. However, since only physical interaction bonding involved in POBUA matrix there is no significant effect was observed on hardness index value between coating POBUA + 0.5 wt. % graphene oxide and POBUA + 0.5 wt. % graphite. Temporarily Gel content value in table 1 explained that all samples achieved similar percentage of polymerisation after 6 passes of UV irradiation which verify that graphite and graphene oxide did not react as radical scavenger. In this parameter study, graphite is considered inert and stable due to carbon atoms layers which arranged in a hexagonal lattice and held together by weak van der Waals forces thus prevent it to interact with any radical element [14] Meanwhile low concentration of graphene oxide particles in POBUA make it ineffective as radical scavenger.

POBUA

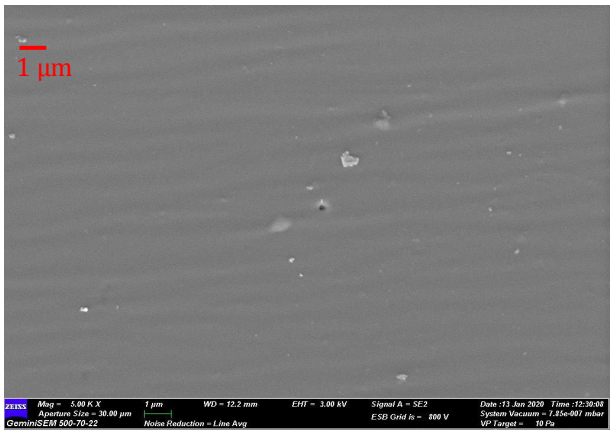

POBUA 0.5 wt. % graphite

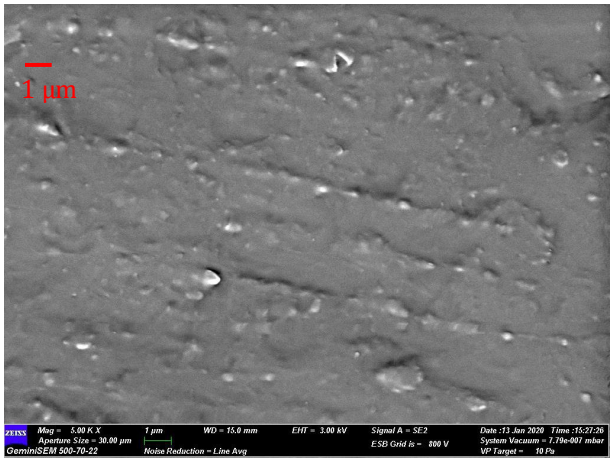

POBUA + 0.5 wt. % graphene oxide

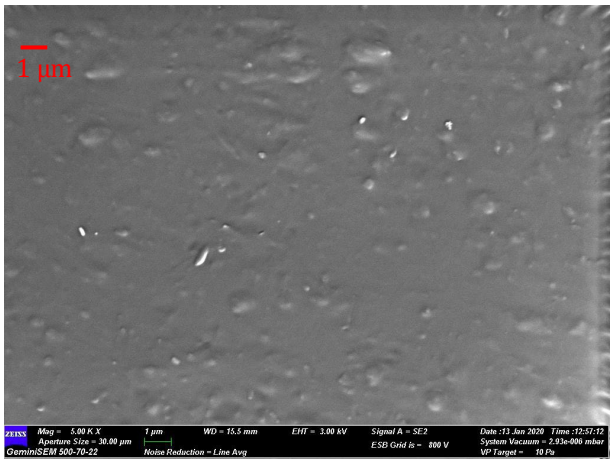

Figure 2. FESEM of POBUA, POBUA +0.5 wt % graphene oxide and POBUA + 0.5 wt % graphite.

3.2 Effect of Graphite and Graphene Oxide Particles on Crystallinity and Morphology

For the purpose of examining the behavior of the polymer matrix, the composition region information of the polymerized material is crucial. In this work X- Ray diffraction analysis was carried out to investigate the POBUA matrix region with presence of graphite and graphene particles. Figure 2 shows the XRD spectrum of POBUA, POBUA + Graphene oxide 0.5 wt. % and POBUA + Graphite 0.5 wt. %. The POBUA coating crystallinity region was increased with presence of graphite and graphene oxide particles. The region with the highest crystallinity was observed in POBUA containing 0.5 wt. % graphite. Graphite particles are typically rigid and have a layered structure [15], [16]. The dispersion of graphite within the polymer will contribute to polymer reinforcement and facilitate polymer molecules to order in more align arrangement to form crystalline structure. This alignment induces a degree of anisotropy (directional orientation) thus enhancing crystallinity region in POBUA matrix. Previous findings reported that the crystallinity of acrylic resin matrix was gradually enhanced by added graphite in polymer [17]. However, the crystallinity region of curable coating for POBUA + Graphene oxide 0.5 wt. % is slightly lower compared to POBUA + Graphite 0.5 wt. % %. The disruption of the crystalline structure of the POBUA was due to formation of hydrogen bonds through interaction between polymer matrix and oxygen from Graphene oxide functional groups. Previous study reported that the increased fraction of hydrogen bonds induced the expansion of crystal lattice due to presence of H-bonds which inhibited the growth of crystalline region [18]. Furthermore large, planar structure of Graphene oxide sheets also leads the steric hindrance and prevents polymer chains from arranging themselves in a crystalline lattice [19].

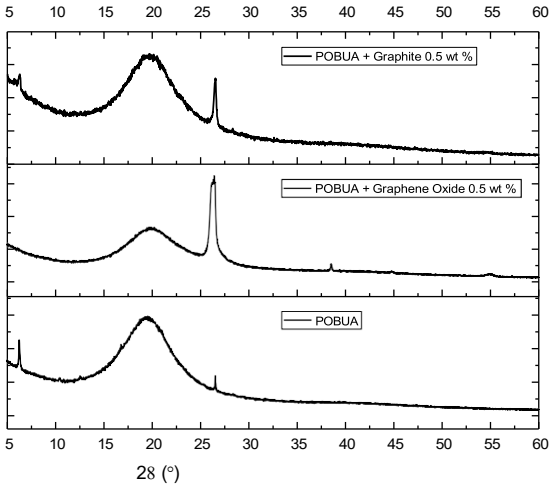

Figure 3. XRD for POBUA, POBUA + 0.5 wt. % graphite, POBUA + graphene oxide 0.5 wt. %.

3.3 Influence of Graphite and Graphene Oxide Particles in Wettability Properties

Contact angle measurements were conducted to assess the impact of graphite and graphene oxide particles on the wettability of the POBUA curable coating. As can be seen from the result in Figure 4 the presence of both particles, depicting the hydrophobicity enhancement on POBUA coating. Polymerisation via UV irradiation on POBUA resin was formed a highly density cross-linked polymer network. This network can create a more impermeable and hydrophobic surface. Crosslinked polymers typically have lower surface energy resulting from the formation of a three-dimensional network of covalent bonds in the polymer matrix. This network reduces the number of available sites for intermolecular interactions with water, making the surface less prone to wetting. This observation was agreeing with the previous study which found that high crosslinked density will increase water contact angle [20]. Moreover, crosslinked polymers are frequently inert and chemically stable, primarily because they are formed by the establishment

of covalent or ionic bonds that link polymer chains, creating an interconnected network. [21]. The construction of polymerized polymer chain generally results in increased hardness and chemical resistance.

Figure 4 also elucidate that the presence of both graphite and graphene oxide enhance value of water contact angle from 106.07° to 120.58° and 121.40°. Graphite or Graphene oxide which is attached physically into a UV-curable coating will act as a filler material to impede water penetration. This phenomenon can be attributed to the pores in the surface coating being filled, leading to an enhancement in surface smoothness and polymer construction. Conversely, a dense surface is achieved when a substantial quantity of graphite is employed. This will reduce the contact area between the water droplet and the coating surface and subsequently increases the contact angle value.

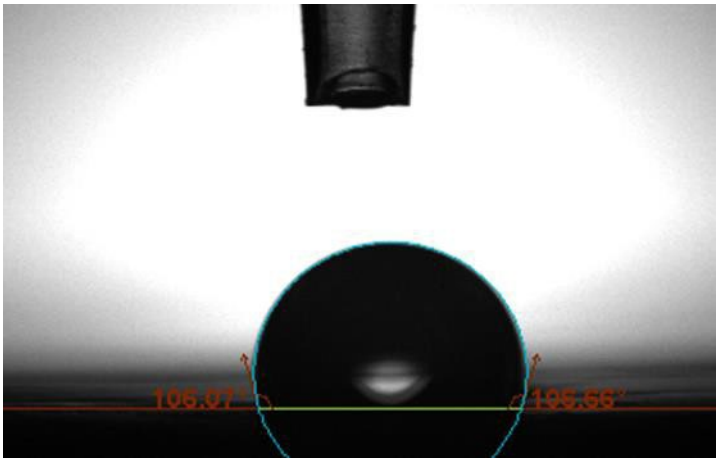

POBUA

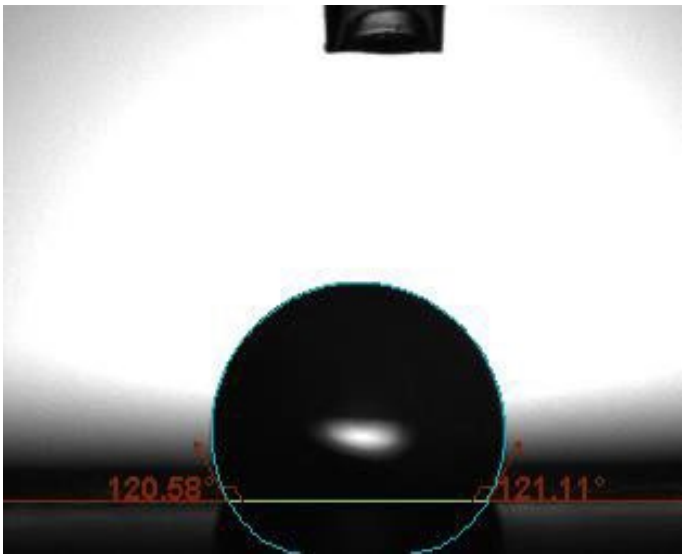

POBUA+ Graphite 0.5 wt. %

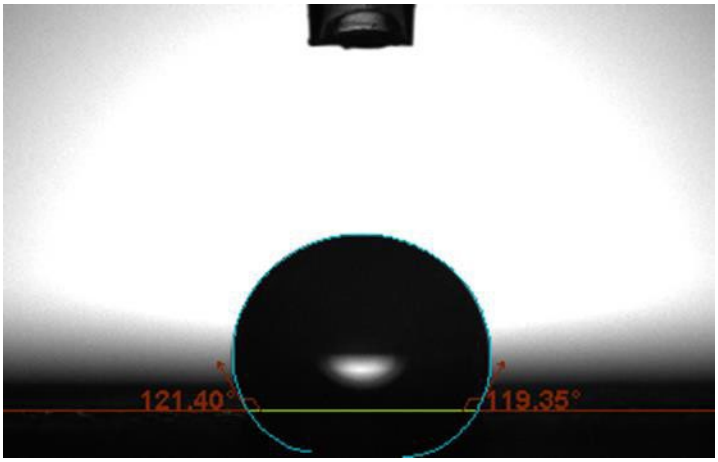

POBUA+ Graphene Oxide 0.5 wt. %

Figure 4. Contact angle for POBUA, POBUA + 0.5 wt. % graphite, POBUA + graphene oxide 0.5 wt. %.

3.4 Effect of Graphite and Graphene Oxide Particles on Corrosion Protection Properties

In this study, electrochemical impedance spectroscopy (EIS) data was extracted to understand the role of graphite and graphene oxide particles in corrosion protection coating. Figure 5 represents the electrical circuit which is applied for fitting the EIS spectra of protective polymer coating [22]. The resulting data produced several parameters, including solution resistance (Rs), resistance of the POBUA-composite rich coating (Rcoat), charge transfer (corrosion) resistance (Rct), capacitance of the POBUA-composite coating (Qc), and electric double layer capacitance (Qdl). Figure 6 visually presents the Nyquist fitted plots, illustrating the corrosion resistance performance of mild steel coated with plain POBUA and POBUA coatings containing 0.5 wt.% graphite and 0.5 wt.% of graphene oxide particles. Each fitted plot displays two-time constants, indicating the presence of corrosion below the coating. These graphs indicate that the electrolyte has permeated through pores, while the second time constant at lower frequencies signifies the corrosion process [23]. Regarding on Table 3, the highest values of Rc (coating resistance) is 30.12 x 10^6 Ωcm^2 which observed for POBUA coatings containing 0.5 wt.% Graphene oxide, while the POBUA coating with 0.5 wt.% Graphite recorded an Rc value of 6.448 x 10^6 Ωcm^2. Meanwhile Rct value also exhibited a similar trend, the highest value was captured for the POBUA coatings + 0.5 wt.% graphene oxide with 260.5 x 10^6 Ωcm^2, followed by POBUA coatings + 0.5 wt.% graphite and POBUA respectively with value 9.253 x 10^6 Ωcm^2 and 2.528 x 10^6 Ωcm^2. It was clearly shown that the presence of Graphene oxide and graphite particles in POBUA coating led to larger semicircles in the Nyquist plots compared to Nyquist semicircle in POBUA coating. This indicates both particles enhanced corrosion protection coating ability compared to the plain POBUA coatings. The Rct value explains the contribution of particles to mild steel corrosion protection. Initially, with low Qc values representing water diffusion, the Rct value is high. However, after electrolyte infiltration, the Rct value decreases due to charge transfer activity on the mild steel surface. The presence of graphene oxide and graphite in the POBUA matrix impedes the penetration of corrosive agents from the electrolyte to the mild steel surface and lengthens the diffusion path. This is evident in the growing radii of the Nyquist semicircles. The percentage of corrosion protection can be calculated using Equation 2 as follows:

$$Protection\ (\%) = \frac{R_{ct} - R_{ct0}}{R_{ct}} \times 100 \qquad (2)$$

where
Rct = charge transfer graphite /graphene oxide POBUA coating,
Rct0 = charge transfer neat POBUA coating

Table 2 also indicates the corrosion protection percentage improved by adduction of graphene oxide and graphite in POBUA resin. Cured coating of POBUA + 0.5 wt % graphene oxide give the highest protection value up to 99.64 % compared with POBUA + 0.5 wt% graphite and neat POBUA cured coating respectively with value 90% and 63.6%. From the result there are 3 main factor which make graphene oxide is better than graphite as filler for corrosion protection:

i. Graphene oxide contains oxygen functional groups (e.g., hydroxyl and carboxyl groups) on its surface, which can introduce polar interactions and promote better adhesion to the polymer matrix. Graphite particles typically lack these oxygen groups and may not bond as effectively with the polymer [24].

ii. Graphene oxide is generally more dispersible in various solvents and polymer matrices compared to graphite particles. Its high surface energy and oxygen-containing groups facilitate better dispersion, leading to a more uniform distribution within the coating. In contrast, graphite particles may agglomerate, creating regions of uneven distribution that can affect coating properties [25].

iii. Graphene oxide has a layered structure with oxygen functional groups that can act as barriers to prevent the dispersion of corrodent agents such as OH and Cl- through the coating. This barrier effect can enhance the overall corrosion resistance of the coating by slowing down or inhibiting the penetration of corrosive substances [26].

The corrosion resistance of POBUA coating films was also assessed using the Tafel extrapolation. Figure 6 shows Tafel polarization curves for the POBUA coatings, demonstrating the effectiveness of the curable coating on mild steel. Results in Table 4 revealed, both graphene oxide and graphite particles were successful increased corrosion potential value of coated mild steel. The presence of graphene oxide and graphite particles reduced the tendency of mild steel to corrode. This contributed by matrix polymer barrier which developed from crosslink network formation. Furthermore, TAFEL plot exhibited that corrosion potential value of POBUA coating were shifted to positive region as graphene oxide or graphite particles added on to POBUA resin. In addition, when graphene oxide and graphite particles are included in the POBUA matrix, the value of current density also decreases, this due to difficulty of mild steel to dissolved thus generate less current density and moved the TAFEL plot to left side. POBUA coating with concentrations of 0.5 wt.% graphene oxide give the best performance of corrosion rate per year (43.91×10^{-6}). Good distribution of graphene oxide in POBUA matrix contributed to the effectiveness of graphene oxide to avoid the corrodent agent pathway beneath the coating. The oxygen-functionalized graphene oxide may introduce tortuous pathways within the coating matrix, making it more challenging for corrosive agents to reach the metal substrate. Oxygen- containing functional groups (e.g., hydroxyl, epoxy, carboxyl groups) on its surface can interact with the surrounding polymer matrix and create barriers thus hindering the movement of corrosive agents. The oxygen-functionalized graphene oxide may introduce tortuous pathways within the coating matrix, making it more challenging for corrosive agents to reach the metal substrate. Oxygen-containing functional groups (e.g., hydroxyl, epoxy, carboxyl groups) on its surface can interact with the surrounding polymer matrix and create barriers thus hindering the movement of corrosive agent [27]. Furthermore, Graphene oxide has a layered structure with oxygen functional groups that can act as barriers to prevent the dispersion of corrodent agents such as OH and Cl- through the coating. This barrier effect can improve corrosion prevention of the coating by slowing down or inhibiting the penetration of corrosive substances [28].

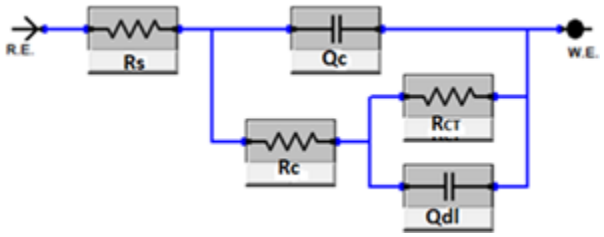

Figure 5. Equivalent circuit nfor the one time contant system. Rs: Solution Resistance, Rc coating resistant, Qc Coating capacitance.

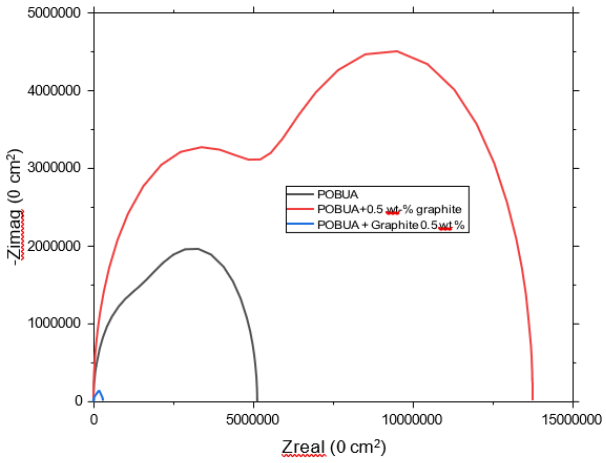

Figure 6. Nyquist fitted plots of POBUA, POBUA+0.5 graphene oxide and POBUA + 0.5 graphite.

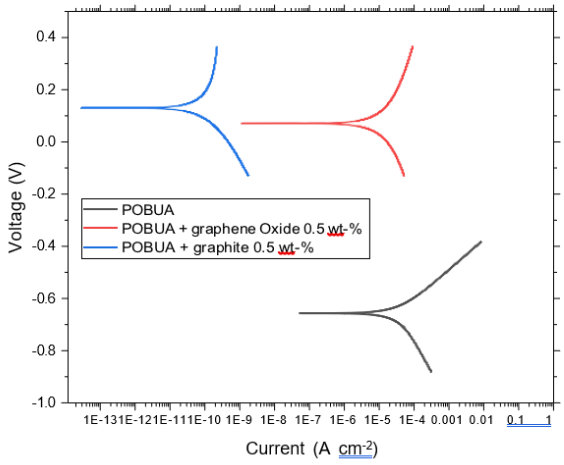

Figure 7. TAFEL plot of POBUA, POBUA +graphene Oxide 0.5 wt. % and POBUA +graphite 0.5 wt.%.

Table 3 Parameter extracted from EIS data of POBUA, POBUA + graphene oxide 0.5 wt. % and POBUA+ graphite 0.5 wt. %

Sample	Rc (10^6) [Ωcm]	Rct (10^6) [Ωcm]	Qc (10^{12}) [Fcm^{-2}]	Qdl (10^{-9}) [Fcm^{-2}]	Corrosion protection [%]	Chi-square (10^4)
Mild steel	8.77	0.92				
POBUA	2.579	2.528	84.28	0.417	63.6	3.82
POBUA+ graphite 0.5 wt%	6.448	9.253	76.35	15.07	90	5.5
POBUA+ graphene oxide 0.5 wt%	30.12	260.5	68.78	111.8	99.64	5.5

Table 4 Tafel plot for POBUA, POBUA + 0.5 wt. % graphite, POBUA + graphene oxide 0.5 wt. %

Sample	Icorr (Acm^{-2})	Ecorr (mv)	CR (mpy)
Mild Steel	102 x 10^{-6}	-683.0	31.24
POBUA	37.8 X 10^{-6}	-658.0	11.57
POBUA + Graphite 0.5 wt.%	273.0 X 10^{-12}	130	125.1 X 10^{-6}
POBUA + Graphene oxide 0.5 wt.%	273.0 X 10^{-12}	95.71	43.91 X 10^{-6}

4. CONCLUSION

UV-curable polyurethane palm oil-based coatings formulated with graphene oxide filler appear to offer superior corrosion protection compared to those containing graphite filler. The presence of graphene oxide particles enhances dispersion, and the barrier effect within the coating, leading to higher charge transfer resistance and improved resistance to corrosion. Formulation of palm oil-based polyurethane UV curable with graphene oxide filler demonstrates higher potential for corrosion protection, especially in environments prone to corrosion.

ACKNOWLEDGMENTS

The primary author wishes to express gratitude to the Malaysia Public Services Department (JPA) for funding the author's education. Additionally, the Ministry of Education Malaysia is acknowledged for their financial support through research grant FRGS/1/2020/TK0/UKM/02/35. The authors would also like to extend their sincere appreciation to the Malaysian Nuclear Agency for their provision of equipment and technical support, which were instrumental in making this work achievable.

REFERENCES

[1] Kaur, R., Singh, P., Tanwar, S., Varshney, G., Yadav, S., Macromol. vol 2 issue 3(2022) pp.284-314.
[2] Suthar, V., Asare, M. A., de Souza, F. M., Gupta, R. K., Polymers. vol 14 issue 22 (2022) p.4974.

[3] Ibrahim, S., Ahmad, A. Mohamed, N. S., Bulletin of Materials Science. Vol 38 issue 5(2015) pp.1155- 1161.
[4] Patil, A. M., Jirimali, H. D., Gite, V. V., Jagtap, R. N., Progress in Organic Coatings. vol 149(2020) p.105895.
[5] Nardeli, J. V., Fugivara, C. S., Taryba, M., Montemor, M. F., Benedetti, A. V., 2021. Chemical Engineering Journal. vol 404(2021) p.126478.
[6] Cao, Y., Liu, Z., Zheng, B., Ou, R., Fan, Q., Li, L., Guo, C., Liu, T., Wang, Q., Composites Part B: Engineering. vol 200 (2020), p.108295.
[7] Deng, H., Xie, F., Shi, H., Li, Y., Liu, S., Zhang, C., Chemical Engineering Journal. vol 446 (2022) p.137124.
[8] Alias, M. S., Othman, N. K., Kamarudin, S. R. M., Harun, M. H., Mohamed, M., Saidin, N. U., Mohamad, S. F., Samsu, Z., Industrial Crops and Products. vol 187 (2022) p.115436.
[9] Leng, Z., Li, T., Wang, X., Zhang, S., Zhou, J., Coatings. vol 12 issue 4(2022) p.434.
[10] Ma, Y., Ye, Y., Wan, H., Chen, L., Zhou, H., Chen, J., 2020. Progress in Organic Coatings. vol 141(2020) p.105547.
[11] Ramezanzadeh, B., Niroumandrad, S., Ahmadi, A., Mahdavian, M., Moghadam, M. M., Corrosion Science. vol 103(2016) pp.283-304.
[12] Salih, A. M., Ahmad, M. B., Ibrahim, N. A., Dahlan, K. Z. H. M., Tajau, R., Mahmood, M. H., Yunus, W. M. Z. W., Molecules. vol 20 issue 8(2015) pp.14191-14211.
[13] Lukhi, M., Kuna, M., Hütter, G., International Journal of Fatigue. vol 113(2018) pp.290-298.
[14] Sengupta, R., Bhattacharya, M., Bandyopadhyay, S., Bhowmick, A.K., Progress in polymer science. vol 36 issue 5(2011) pp.638-670.
[15] Kausar, A., Avant-Garde Polymer and Nano-Graphite-Derived Nanocomposites Versatility and Implications. C. vol 9 issue 1(2023) p.13.
[16] Liebscher, M., Domurath, J., Saphiannikova, M., Mueller, M.T., Heinrich, G., Poetschke, P., Polymer. vol 200 (2020) p.122577.
[17] De León, A. S., Molina, S. I., Polymers. vol 12 issue 5(2020) p.1103.
[18] Górecka, Ż., Idaszek, J., Kołbuk, D., Choińska, E., Chlanda, A., Święszkowski, W., Materials Science and Engineering: C. vol 114 (2020) p.111072.
[19] Zheng, W., Shen, B., Zhai, W., New progress on graphene research. vol 10(2013) p. 50490.
[20] Clemens, A. L., Jayathilake, B. S., Karnes, J. J., Schwartz, J. J., Baker, S. E., Duoss, E. B., Oakdale, J. S., Polymers. vol 15 issue 6(2023) p.1534.
[21] Osman, B., Aydemir, T. G., Materials Research Express. vol 6 issue5 (2019) p.055008.
[22] Hernández, H. H., Reynoso, A. R., González, J. T., Morán, C. G., Hernández, J. M., Ruiz, A. M., Hernández, J. M., Cruz, R. O., Electrochemical Impedance Spectroscopy. (2020), pp.137-144.
[23] Suleiman, R. K., Kumar, A. M., Adesina, A. Y., Al-Badour, F. A., Meliani, M. H., Saleh, T. A., Corrosion Science. Vol 169(2020) p.108637.
[24] Sharma, N., Sharma, S., Anticorrosive coating of polymer composites: A review. Materials Today: Proceedings, 44, (2021) pp.4498-4502.
[25] Paredes, J. I., Villar-Rodil, S., Martínez-Alonso, A., Tascon, J. M., Langmuir. vol 24 issue 19(2008) pp.10560-10564.
[26] Tang, S., Lei, B., Feng, Z., Guo, H., Zhang, P., Meng, G., Coatings. vol 13 issue 6 (2023) p.1120.
[27] Montemor, M. F., Surface and Coatings Technology. vol 258 (2014) pp.17-37.
[28] Di, H., Yu, Z., Ma, Y., Zhang, C., Li, F., Lv, L., Pan, Y., Shi, H., He, Y., Journal of the Taiwan Institute of Chemical Engineers. vol 67(2016) pp.511-520.